

Probing omics data via harmonic persistent homology *

Davide Gurnari^{1†}[0000-0002-3668-8711], Aldo Guzmán-Sáenz^{2†}[0000-0003-2725-621X], Filippo Utró²[0000-0003-3226-7642], Aritra Bose²[0000-0002-8665-056X], Saugata Basu³[0000-0002-2441-0915], and Laxmi Parida²[0000-0002-7872-5074]

¹ Dioscuri Centre in Topological Data Analysis, Mathematical Institute PAN, Warsaw, PL

² IBM Research, Yorktown Heights, NY, USA

³ Dept. of Mathematics, Purdue University, West Lafayette, IN, USA

parida@us.ibm.com

Abstract. Identifying molecular signatures from complex disease patients with underlying symptomatic similarities is a significant challenge in analysis of high dimensional multi-omics data. Topological data analysis (TDA) provides a way of extracting such information from the geometric structure of the data and identify multiway higher-order relationships. Here, we propose an application of *Harmonic* persistent homology which overcomes the limitations of ambiguous assignment of the topological information to the original elements in a representative topological cycle from the data. When applied to multi-omics data, this leads to the discovery of hidden patterns highlighting the relationships between different omic profiles, while allowing for common tasks in multiomics analyses such as disease subtyping, and most importantly biomarker identification for similar latent biological pathways that are associated with complex diseases. Our experiments on multiple cancer data show that *harmonic* persistent homology and TDA can be very useful in dissecting multi-omics data and identify biomarkers while detecting representative cycles of the data which also predicts disease subtypes.

Keywords: Topological Data Analysis · Pattern Discovery · Data Analysis.

*Supported by IBM Research

†These authors contributed equally to this work

1 Introduction

Omics studies have gained substantial importance to unravel interactions between biomarkers underlying complex diseases with the availability of data from different modalities due to technological advances [5]. These biomarkers are instrumental in clinical decision-making and drug discovery. Although extracting them from complex data can often be a challenge with the high dimensionality of the datasets as well as heterogeneous molecular profile of patients and disease subtypes and other biases that plague epidemiological studies [9]. Furthermore, identifying biomarkers that exhibit similar underlying biological pathways or molecular profiles among patients can be an even bigger impediment and still need investigation and novel analysis approaches. One of the most robust approaches that analyze data under a new perspective is Topological Data Analysis (TDA). TDA has been shown as a useful tool for the analysis of omics data [2,3,8,17,16,12,11], and it allows to identify (complex) multiway high order relationship in the data.

Persistent homology is a tool from TDA used to study the topology of spaces at different scales with algebraic constructs. This approach has been used successfully in the context of pattern discovery (see for example [2]). One limitation of this approach is that there is an inherent ambiguity when mapping back the information obtained from the topology of a space (say the geometric realization of a simplicial complex) to the basic elements (in this case the vertices of the simplicial complex). In this paper we overcome this problem by applying a new tool introduced in [1] – namely *Harmonic* Persistent Homology. Use of harmonic persistent homology yields an unambiguous way to select representative cycles from homology classes which furthermore satisfy certain theoretical guarantees (simplices which are essential for this class appear with highest weight). Use of harmonic homology thus overcomes a basic obstacle for the use of TDA in the context of genomic data analysis, where identifying important simplices (which encodes biologically relevant relationships) is crucial. Although TDA and persistent homology has been applied in analyzing multiomics data [8,16,17], they were different in scope as they simply used persistent homology to identify spatial patterns in multiomics data and were plagued by the aforementioned issue of mapping the learned topological structure back to the elements or vertices in the simplicial complex. We perform computation of persistent harmonic cycles with our software library, called `maTilda`, available at <https://github.com/IBM/matilda>.

Intuitively, harmonic persistent homology enables us to establish relationships between features or points in the data, that could lead to discovery of hidden patterns and/or novel insights thanks to the capability of TDA to analyze data at different scales. Moreover, harmonic persistent homology is naturally equipped to analyze high order interactions between data points, allowing us to explore beyond simple pairwise interactions by analyzing homological features in dimensions higher than one. A schematic of our framework is given in Figure 1. In this manuscript, we show how harmonic persistent homology brings to light relationships and deeper comprehension of biological data that can help generate new hypothesis using multi-omics data. Due to the absence of methods and data which addresses the precise problem, it is hard to perform a benchmark comparison of the different tools reported in literature. Therefore, in this manuscript, we demonstrate the capability of harmonic persistent homology by reproducing and expanding on known results from the literature. In particular, using different datasets such as RNA from CLL patients [7], scRNA data [10], and multi-omics data from The Cancer Genome Atlas (TCGA) database⁴, we validate the patterns found by our framework using external clinical knowledge and expected baseline patterns.

Roadmap. In the next section we give the mathematical underpinnings for the essential simplices and harmonic persistent homology. In Section 3, we apply our framework to different datasets and summarize the results.

2 Methods

The goal of this section is to provide the mathematical background for our Harmonic Framework. In Section 2.1 we recall some basic definitions from simplicial homology theory. The interested reader is directed to [4] for a more in depth background on Topological Data Analysis. We define Harmonic Homology in Section 2.2 and introduce Harmonic Persistent Homology in Section 2.3. We explain the relation between essential simplices and the harmonic representative in Section 2.4 and provide a toy example in Section 2.5. Finally, we describe how to apply this framework to real-world data in Section 2.6.

⁴<https://www.cancer.gov/tcga>

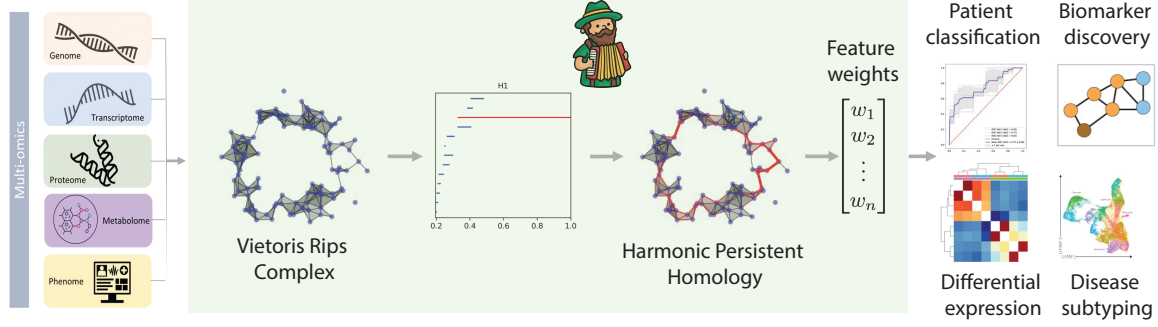


Fig. 1: Schematic of the Harmonic Framework. Given a set of multi-omic samples, the algorithm builds a topological structure on top of the input data according to a predefined similarity measure; and computes its persistent homology barcode. A subset of bars is selected from the barcode and their corresponding harmonic representatives are computed. The harmonic representative corresponding the red bar in the diagram is depicted in red in panel 4, edges' thickness are proportional to their harmonic weights. Harmonic weights on the simplices (e.g. edges) can then be converted to weights on the samples and used as feature vectors for a series of downstream tasks (we limit ourselves to report a few).

2.1 Simplicial complex and boundary maps

Definition 1. A finite simplicial complex K is a set of ordered subsets of $[N] = \{0, \dots, N\}$ for some $N \geq 0$, such that if $\sigma \in K$ and τ is a subset of σ , then $\tau \in K$.

Notation 1 If $\sigma = \{i_0, \dots, i_p\} \in K$, with K a finite simplicial complex, and $i_0 < \dots < i_p$, we will denote $\sigma = [i_0, \dots, i_p]$ and call σ a p -dimensional simplex of K . We will denote by $K^{(p)}$ the set of p -dimensional simplices of K .

Definition 2 (Chain groups and their standard bases). Suppose K is a finite simplicial complex. For $p \geq 0$, we will denote by $C_p(K) = C_p(K, \mathbb{R})$ (the p -th chain group), the \mathbb{R} -vector space generated by the elements of $K^{(p)}$, i.e.

$$C_p(K) = \bigoplus_{\sigma \in K^{(p)}} \mathbb{R} \cdot \sigma.$$

The tuple $(\sigma)_{\sigma \in K^{(p)}}$ is then a basis (called the standard basis) of $C_p(K)$ (where by a standard abuse of notation we identify σ with the image of $1 \cdot \sigma$ under the canonical injection of the direct summand $\mathbb{R} \cdot \sigma$ into $C_p(K) = \bigoplus_{\sigma \in K^{(p)}} \mathbb{R} \cdot \sigma$).

Definition 3 (The boundary map). We denote by $\partial_p(K) : C_p(K) \rightarrow C_{p-1}(K)$ the linear map (called the p -th boundary map) defined as follows. Since $(\sigma)_{\sigma \in K^{(p)}}$ is a basis of $C_p(K)$ it is enough to define the image of each $\sigma \in C_p(K)$. We define for $\sigma = [i_0, \dots, i_p] \in K^{(p)}$,

$$\partial_p(K)(\sigma) = \sum_{0 \leq j \leq p} (-)^j [i_0, \dots, \widehat{i_j}, \dots, i_p] \in C_{p-1}(K),$$

where $\widehat{}$ denotes omission.

One can easily check that the boundary maps ∂_p satisfy the key property that

$$\partial_{p+1}(K) \circ \partial_p(K) = 0,$$

or equivalently that

$$\text{Im}(\partial_{p+1}(K)) \subset \ker(\partial_p(K)).$$

Notation 2 (Cycles and boundaries) We denote

$$Z_p(K) = \ker(\partial_p(K)),$$

(the space of p -dimensional cycles) and

$$B_p(K) = \text{Im}(\partial_{p+1}(K))$$

(the space of p -dimensional boundaries).

Definition 4 (Simplicial homology groups). The p -dimensional simplicial homology group $H_p(K)$ is defined as

$$H_p(K) = Z_p(K)/B_p(K).$$

Note that $H_p(K)$ is a finite dimensional \mathbb{R} -vector space.

2.2 Representing homology classes by harmonic chains

Let K be a finite simplicial complex. We make the chain group $C_p(K)$ into an Euclidean space by fixing an inner product defined by:

$$\langle \sigma, \sigma' \rangle = \delta_{\sigma, \sigma'}, \sigma, \sigma' \in K^{(p)} \quad (1)$$

(i.e. we declare the basis $(\sigma)_{\sigma \in K^{(p)}}$ to be an orthonormal basis).

Definition 5 (Harmonic homology subspace). For $p \geq 0$, we will denote

$$\mathfrak{h}_p(K) = Z_p(K) \cap B_p(K)^\perp.$$

and call $\mathfrak{h}_p(K) \subset C_p(K)$ the harmonic homology subspace of K .

In terms of matrices, we have the following description of $\mathfrak{h}_p(K)$ as a subspace of $C_p(K)$. For $p \geq 0$, let $\mathcal{A}_p(K)$ denote an orthonormal basis of $C_p(K)$ (for example, if the chosen inner product is the standard one given in (1), then we can take $\mathcal{A}_p(K) = \{\sigma | \sigma \in K^{(p)}\}$). Let $M_p(K)$ denote the matrix of ∂_p with respect to the basis $\mathcal{A}_p(K)$ of $C_p(K)$, and the basis $\mathcal{A}_{p-1}(K)$ of $C_{p-1}(K)$. Then, $\mathfrak{h}_p(K)$ can be identified as the subspace of $C_p(K)$ which is equal to the intersection of the nullspaces of the two matrices $M_p(K)$ and $M_{p+1}(K)^T$. More precisely,

$$z \in \mathfrak{h}_p(K) \Leftrightarrow [z]_{\mathcal{A}_p(K)} \in \text{null}(M_p(K)) \cap \text{null}(M_{p+1}(K)^T). \quad (2)$$

2.3 Persistent Harmonic Homology

Even though the data that we deal with in this paper does not have a geometric origin, in order to visualize the concept of persistent homology it is useful to first consider the case of a point-cloud $S \subseteq \mathbb{R}^n$ that approximates some underlying manifold M . Since we only have access to S , with it we will construct an object that approximates the “shape” of M . To do this, consider n -dimensional balls of radius r centered on elements of S and denote their union by X_r . A well-known result in algebraic topology known as the *Nerve Lemma* assures us that the “shape” of the union of these balls is encoded in a simplicial complex (Definition 1) constructed using intersections of the aforementioned balls (more specifically, we consider the *nerve* of the covering formed by the balls). The choice of radius r is not clear, however, and thus we let it take all values in $[0, \infty)$ while keeping track of “shape” changes in X_r .

As one can easily visualize, as r starts growing from 0, there are many spurious homology classes that are born and quickly die off (e.g. the corresponding holes are filled in) and these have nothing to do with the topology of M . Persistent homology is a tool that can be used to separate this “noise” from the *bona fide* homology classes of M .

The mathematical notion that encapsulates these intuitions is called *Persistent Homology*. For a finite filtered simplicial complex X , that is, a sequence of finite simplicial complexes $\{X_i\}_{1 \leq i \leq n}$ with $X_i \subseteq X_j$ if $i \leq j$ taking only a finite number of different values, we define their *Persistent Homology* of degree p by

$$PH_p(X) = (\{H_p(X_i)\}_{1 \leq i \leq n}, \{\iota_*^{i,j}\}_{i,j \in \{1, \dots, n\}})$$

and their *Persistent Homology Groups* by

$$H_p^{i,j}(X) = \iota_*^{i,j}(X_p)$$

where $\iota_*^{i,j}$ is the morphism in homology induced by the inclusion $X_i \subseteq X_j$.

The structure of $PH_p(X)$ is that of a *persistence module* (which is a graded module over the graded ring of polynomials in one variable). There exists a finite multiset $D = \{(r_1, s_1), \dots, (r_l, s_l)\}$ of pairs satisfying $r_i < s_i$ that encodes the isomorphism class of $PH_p(X)$. The pairs (r_i, s_i) have interpretations as the birth-time and death-time of homology classes that appear in the various $H_p(X_i)$, and is usually called (and displayed as) the *barcode* of the filtration \mathcal{F} (the pairs (r_i, s_i) themselves are referred to as bars of the filtration).

Bars of short length corresponds to noise, while the ones which are long (persistent) reflect the homology of the underlying manifold M . The barcode of the filtration associated to S can be used a feature of S for learning or comparison purposes. In particular, the barcodes of two finite sets S, S' which are “close” as finite metric spaces, are themselves close under appropriately defined notion of distance between barcodes. An example of a filtration with its corresponding barcode is shown in Figure 2.

Notice that the barcode of a filtration (being just a set of ordered pairs of numbers) do not record any information about the underlying simplicial complex – in particular, about the structure and the cycles representing the homology classes whose births and deaths are encoded by the bars. Adding that information is not a trivial task. Strictly speaking homology classes representing bars, are themselves elements of certain sub-quotients of vector spaces spanned by the simplices of the complex – and this introduces an inherent ambiguity in choosing representative cycles to represent bars. The authors of [1] overcome this problem by introducing an extra structure (inner product) on the vector spaces (the so called chain spaces) arising in the definition of homology – and using this inner product there is a canonical choice of cycles (called harmonic cycles) which represent the bars in the persistent bar codes.

It turns out that the harmonic bars have a certain additional property (proved in [1]) which makes them suitable choice as representatives. The harmonic bars put higher weights on simplices that are *essential* – meaning that the simplices that *must* appear with non-zero coefficient in *any* choice of representative cycle for that particular bar. This last property indicates that the weight of the simplices in harmonic representatives of the bars in a bar diagram of filtrations coming from genomic data could carry important information about biological relationships. The main goal of this paper is to understand how far this is true by applying harmonic persistence theory to multiomics data sets and check whether it can perform certain tasks like develop prognostic biomarker signatures in complex diseases prognosis, predicts subtypes and discover biomarkers for accelerating therapeutic discovery.

2.4 Essential simplices and harmonic representative

Given a bar in the persistent barcode of a filtration (arising from some application) it is often natural to ask for a cycle in the cycle space of the simplicial complex representing this bar. However, such cycles are only defined modulo some equivalences – and so there is no unique answer to this question. In applications (see for example [2]) it is also important to associate a set of simplices to a given bar which play the most important role in the birth of the bar. We call this set, the set of essential simplices of the bar (see [1] for a precise definition).

If b is a bar in the barcode of a filtration and z is a cycle representing b , then the set of simplices that appear with a non-zero coefficient in z contains the set of essential simplices of b , but could be larger. One measure of the “quality” of the representing cycle z is the relative weights of the essential and the non-essential simplices appearing in its support. The following quantity was defined in [1] as a measure of this quality.

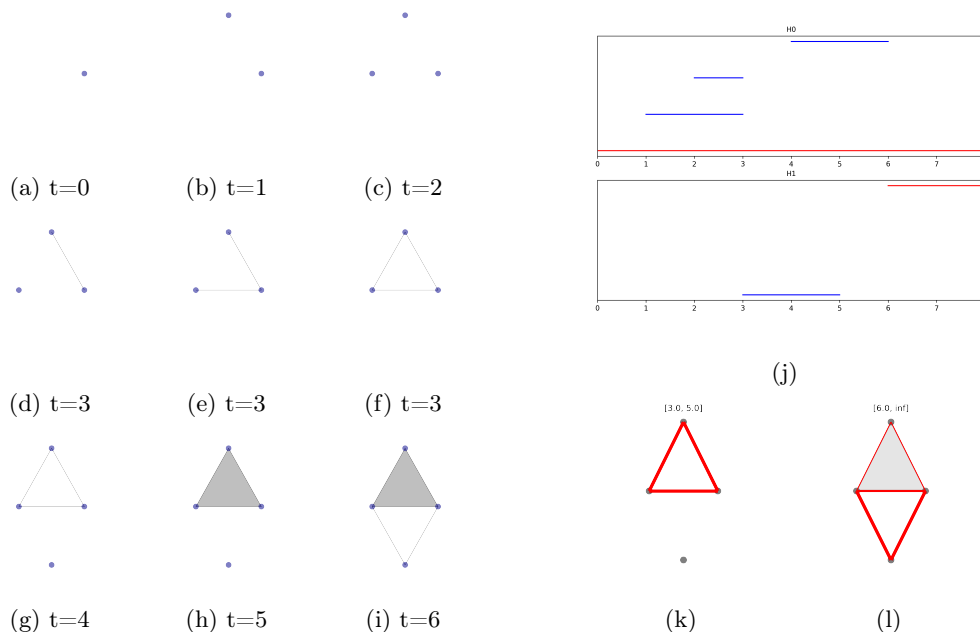


Fig. 2: Example of a filtered simplicial complex and its persistent homology, found in [1]. Figures 2a through 2i illustrate the stages of the filtration, and Figure 2j is the barcode associated to the filtration. Skeleton and barcode plots created using `maTi1DA`. Figures 2k and 2l show harmonic representatives in red, with thickness proportional to the absolute value of coefficients in a chain of a given simplex.

Definition 6 (Relative essential content). Let b be a bar in the barcode of a filtration, and $z = \sum_{\sigma \in K(p)} c_{\sigma} \sigma$ is a cycle representing z . We denote

$$\text{content}(z) = \left(\frac{\sum_{\sigma \in \Sigma(b)} c_{\sigma}^2}{\sum_{\sigma \in K(p)} c_{\sigma}^2} \right)^{1/2}.$$

We will call $\text{content}(b)$ the relative essential content of z .

The following theorem proved in [1] and which justifies our approach in the current paper states that that the relative essential content is maximized by the harmonic representative of a bar.

Theorem 1 (Harmonic representatives maximize relative essential content). With the same notation used above, let z_0 be a harmonic representative of a bar b . Then for any cycle z representing b ,

$$\text{content}(z) \leq \text{content}(z_0).$$

Remark 1. Note that Theorem 1 implies in particular that the relative essential contents of any two harmonic representatives of a simple bar are equal. But this is clear also from the definition of the relative essential content and the fact that any two harmonic representatives of a simple bar are proportional.

2.5 An example

We now discuss an example to clarify the notion of harmonic representatives and essential simplices.

Example 1. Let K be the simplicial complex defined by (see Figure 2 at $t = 6$):

$$\begin{aligned} K^{(0)} &= \{[0], [1], [2], [3]\}, \\ K^{(1)} &= \{a = [0, 1], b = [1, 2], c = [0, 2], d = [0, 3], e = [2, 3]\}, \\ K^{(2)} &= \{t = [0, 1, 2]\}. \end{aligned}$$

The matrices representing the boundary maps ∂_2 and ∂_1 are then as follows.

$$M_2(K) = \begin{matrix} & t \\ a & \begin{bmatrix} 1 \\ 1 \\ -1 \\ 0 \\ 0 \end{bmatrix} \\ b & \\ c & \\ d & \\ e & \end{matrix}, \quad M_1(K) = \begin{matrix} & a & b & c & d & e \\ [0] & \begin{bmatrix} -1 & 0 & -1 & -1 & 0 \\ 1 & -1 & 0 & 0 & 0 \\ 0 & 1 & 1 & 0 & -1 \\ 0 & 0 & 0 & 1 & 1 \end{bmatrix} \\ [1] & \\ [2] & \\ [3] & \end{matrix}$$

The harmonic homology subspace (in dimension one) $\mathfrak{h}_1(K)$ is then the intersection of the null spaces of $M_1(K)$ and ${}^tM_2(K)$, and is equal to the nullspace of the following matrix obtained by concatenating (row-wise) $M_1(K)$ and ${}^tM_2(K)$.

$$\begin{matrix} & a & b & c & d & e \\ \begin{bmatrix} -1 & 0 & -1 & -1 & 0 \\ 1 & -1 & 0 & 0 & 0 \\ 0 & 1 & 1 & 0 & -1 \\ 0 & 0 & 0 & 1 & 1 \\ 1 & 1 & -1 & 0 & 0 \end{bmatrix} & & & & & \end{matrix}$$

We get that $\mathfrak{h}_1(K)$ is equal to the span of the vector whose coordinates are given by the column vector:

$$\begin{matrix} & t \\ a & \begin{bmatrix} 1 \\ 1 \\ 2 \\ -3 \\ 3 \end{bmatrix} \\ b & \\ c & \\ d & \\ e & \end{matrix}$$

Notice that the absolute values of the coordinates corresponding to the basis vectors representing the edges d, e are the greatest. This confirms the intuition that the edges d, e are more significant in the one dimensional homology of K compared to the edges a, b, c . Indeed, the edges d, e must occur with non-zero coefficient in every non-zero 1-cycle representing a non-zero homology class in $H_1(K)$. The same is not true for the other three edges. Such edges were called ‘‘essential simplices’’ in [2].

2.6 Harmonic Weights from Data

We developed the following methodology to extract harmonic weights from multi-omics data, as depicted in Figure 1. Given a collection of samples together with an appropriate notion of distance (euclidean, correlation, cosine, etc.), we build the following structure on top of it and compute its persistent homology barcodes.

Definition 7 (Vietoris-Rips complex). *Let X be a finite collections of points. Given a parameter $\epsilon \leq 0$, the Vietoris-Rips complex constructed from X is the collection of all subset of diameter at most 2ϵ , where the diameter is the greatest distance between any pair of vertices*

$$V-R(X, \epsilon) = \{\sigma \subseteq X \mid \text{diam}(\sigma) \leq 2\epsilon\} \quad .$$

The filtration of each simplex is given by its diameter.

It should be noted that, for too large values of the parameter ϵ , the size of a Vietoris-Rips complex tends to grow exponentially with the number of points. As a matter of fact, it is straightforward to show that for any ϵ larger than the largest distance between any pairs of points; the resulting complex will be fully connected and it will contain 2^n simplices, where n is the number of data points. In order to avoid this exponential explosion, is it common practice to chose a value of ϵ strictly less than the diameter of the whole point cloud.

A possible heuristic for the choice of ϵ is using the maximal distance between any point and its nearest neighbour, in order to assure the existence of only one connected component at the maximum filtration level. For the applications described in Section 3 we choose the minimal ϵ such that all 1-dimensional bars have finite length.

For a given dimension p , usually $p = 1$, we select all the bars in the p -dimensional barcode that are longer than a threshold and compute their harmonic representatives. Such threshold can be determined as a specific quantile of the distribution of the bars' lengths. As mentioned in the previous section, each p -dimensional harmonic representative consist of a linear combination of p -simplices. In particular, each 1-dimensional harmonic representative is a linear combination of edges. The absolute values of the coefficients of such linear combinations are the *harmonic weights*. Harmonic weights take value in the unit interval $[0, 1]$ and they encode how important each simplex is for a given cycle; in particular, all essential simplices have weight 1.

Since each p -dimensional simplex corresponds to a collection of $(p + 1)$ data points⁵, we can assign weights to the datapoints themselves by considering for each node in the Vietoris-Rips complex, the sum of the weights of its cofaces. For example, given a 1-dimensional harmonic representative, we can translate the weights from the edges to the nodes by assigning to each node the sum of the weights of its adjacent edges.

3 Results and Discussion

In this section, we are going to showcase some possible applications of harmonic persistent homology in multiomics data. We analyze a few public datasets with different omic profiles such as transcriptomics, DNA methylation, single cell RNAseq, as well as, drug resistance to highlight how our framework is able to capture intrinsic and hidden features in the data. In particular, Sections 3.1 and 3.3 the weight of the edges are considered, while Sections 3.2 and 3.4 the weight on the nodes are considered (as described in Section 2.6).

3.1 Harmonic persistent homology predicts disease subtypes

We analyzed gene expression data of 958 samples from TCGA, comprising of 561 Luminal A, 207 Luminal B and 190 basal-like breast cancer samples. We then selected key genes differentially expressed for the Luminal A subtype and the basal-like subtype indicated in [6]. For each pair of subtypes, LumA-Basal, LumB-Basal, LumA-LumB, we sampled 150 samples for each subtype (to ensure class balance) and built a Vietoris-Rips complex using distance correlation [14] as metric between the samples, interpreted as points in a 16 dimensional gene space. We then selected all bars in the 1-dimensional persistence barcodes having length greater than 0.08 (threshold is determined as explained in Section 2.6 using the 0.97 quantile) and computed their harmonic representatives. For each representative, we computed the sum of the harmonic weights for each edge, defined by the labels of its two (or three) nodes (e.g. LumA-LumA or LumA-Basal or LumA-LumB-Basal) as shown in Figure 3. Our harmonic persistent homology framework is able to quantify the expected differences in gene expressions levels between samples of the same subtype as we selected key differentially expressed genes prior to computing their harmonic weights. Hence, our framework plays an instrumental role in prediction of disease subtypes.

3.2 Application in multi-omics analysis

In order to demonstrate how our framework can tackle multi-omics data we analyzed a set of 690 breast cancer samples from the TCGA database for which both RNAseq and Methylation450 data are present. The dataset is comprised of 414 Luminal-A, 141 Luminal-B and 135 basal-like samples, and we considered 28495 genes and 363791 methylation sites for a total of 392286 features. We concatenated the RNAseq and Methylation450 data and projected them to a 100-dimensional space using PCA. We built a Vietoris-Rips complex using distance correlation and computed its 1-dimensional persistent homology up to a maximum filtration value of 0.75. We then computed the harmonic representatives of all 66 bars longer than 0.07 (0.97 quantile) For each representative we extracted the harmonic weights on the samples. By doing so we obtained a 690×66 weights matrix, depicted in Figure 4a. Single-linkage clustering on the samples' weights revealed a large cluster of mostly basal-like samples, whose characteristic are shown in Figure 4b. It

⁵Recall that points are 0-dimensional simplices, edges are 1-dimensional, etc.

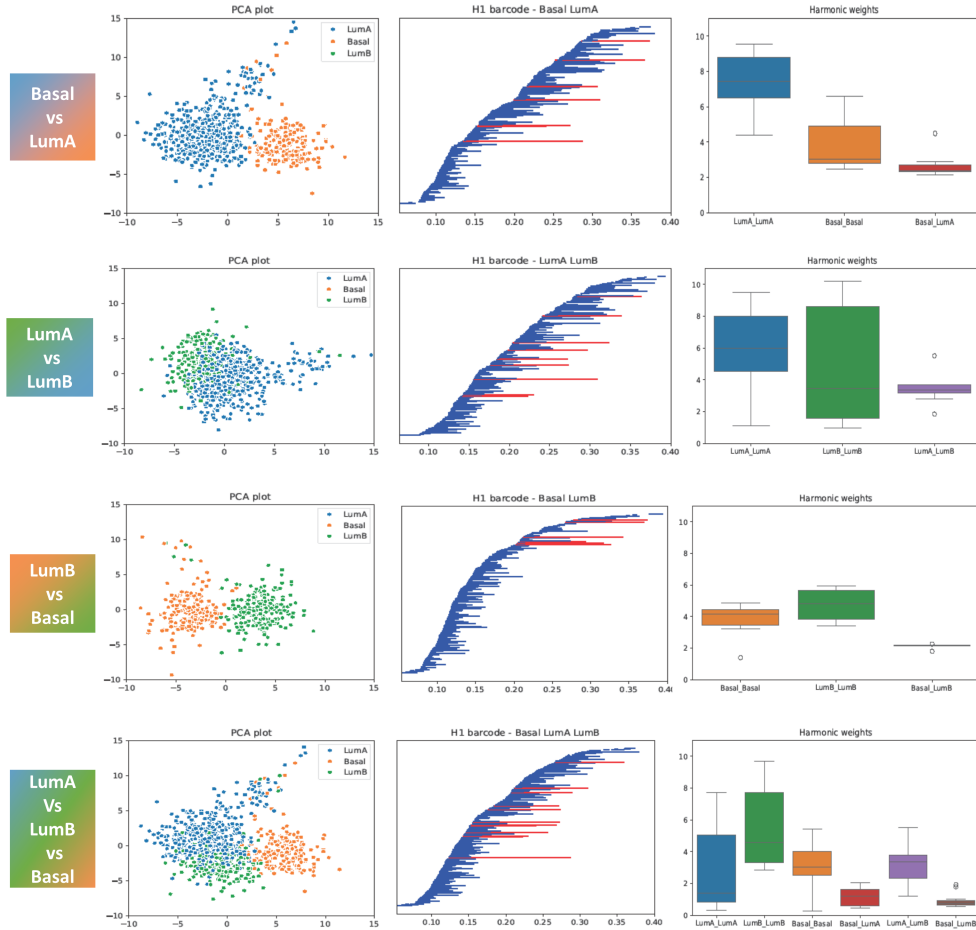


Fig. 3: Harmonic persistent homology distinguishes between breast cancer subtypes (a) PCA plot, (b) 1-dimensional barcode, and (c) distribution of the cumulative harmonic weights for possible pairs of subtypes. The red colored lines in (b) indicate the bars longer than 0.08 for which the harmonic representatives were computed.

is important to notice that this cluster has been found by our method without any knowledge of the nine descriptors shown on top of Figure 4a, relying solely on the combined RNA and methylation data. These additional information can then be used to eternally validate our findings and show how different harmonic cycles capture interactions between different subsets of data. At the same time, harmonic cycles with similar weights cluster together samples with similar descriptors. This approach could then be used on other datasets and lead to the discover of new subgroups of patients along with new markers/findings for these subgroups.

3.3 Discovery of disease transition using Single cell RNA data

We also perform our analysis on single cell RNA data from lymphnode of a cancer under transformation to an high-grade malignancy and rapid disease progression [10]. In particular, Richter syndrome (RS), is an aggressive lymphoma developing in patients with chronic lymphocytic leukemia (CLL). The sample was analyzed with fluorescence activated cell sorting to identify CLL and RS cell. As reported in the original paper that describe the data, the sample shows a strong mixture CLL and RS cell (as shown in Fig 5A). Most likely the sample was collected in an early trasformation stage. We compute the Harmonic persistent homology on a sample of 400 random cell (200 per type) in order to avoid possible class bias. Multiple runs were performed for stability of the results, and a random subset of results are shown in Fig 5B-D. In particular we can see how the cycles capture the two different cell cycles. In particular, further study about

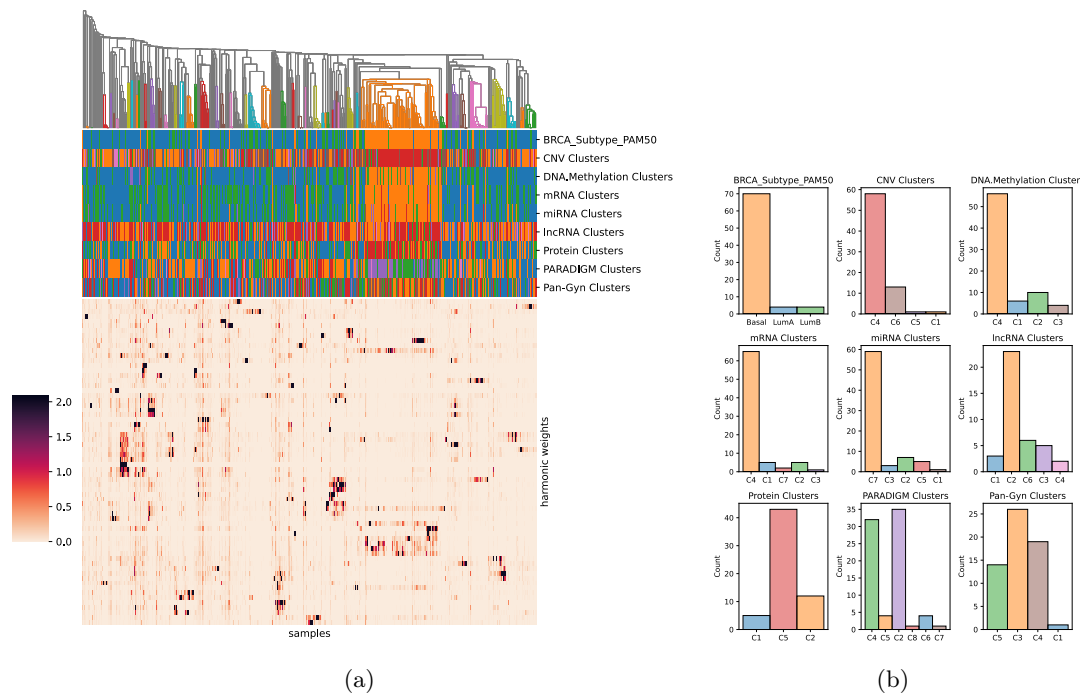


Fig. 4: Single-linkage hierarchical clustering of breast cancer samples using harmonic weights is able to detect a large basal-like cluster, depicted in orange in (a). The distributions of different descriptors for samples in this cluster are shown in (b).

of the cells involved in edges with mix label could shed some lights to the understanding of this aggressive disease and the cause of the transition from CLL to RS.

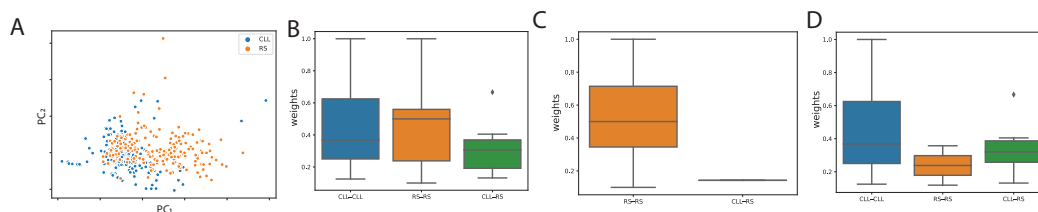


Fig. 5: A. PCA of the 400 random cells from scRNA. B weights distribution of the longest cycles. C and D distribution of the weights in the first two longest cycles

3.4 Transcriptomic discovery associated with treatment progression

We consider transcriptomic data of 11 CLL patients that were treated with Venetoclax (a BCL2 inhibitor) discussed in [7] for which RNA data were collected pre and post treatment at which the patient was progressing. We selected 98 genes that are known to CLL (see Section S1 for the full list) and provided as input to our harmonic framework the two time-points cohort independently to show the capability that our tool to extract insight about the data with less amount information. It is worth pointing out that due to the limited size of the cohort classical approaches, e.g. machine learning, cannot be applied. For completeness we also consider the two cohort together and compared with a standard differential expression analysis performed in [7] and found in common some important genes like NOTCH1, NFKB2 and HIST1H1B and pathways as reported later.

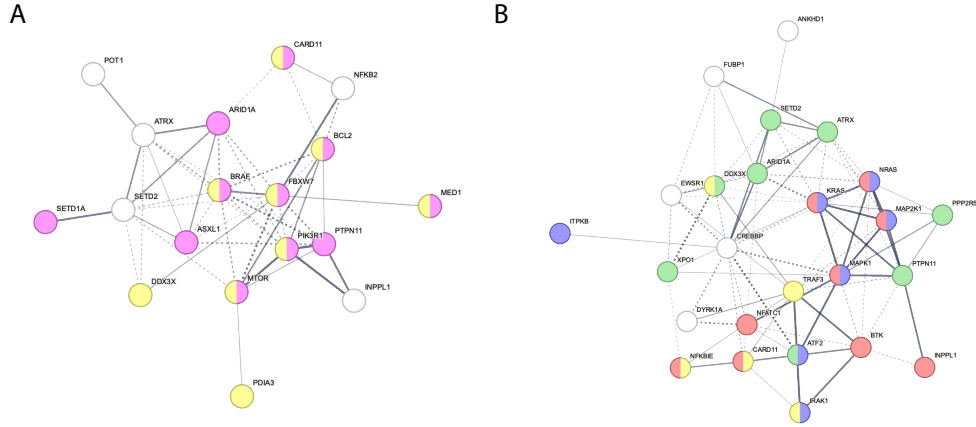


Fig. 6: String network of the identified genes. The edges indicate both function and physical association. Edge color indicates the type of interaction evidence. A Genes set for the pre-treatment cohort. B Gene set for the post-treatment cohort.

The identified genes in each of the two cohort used for a String DB network [13] analysis (see Fig 6) to analyze protein-protein interactions of the identified genes in samples from Venetoclax cohort at pre-treatment and progression time points. At pre-treatment timepoints, there was significant enrichment of genes in the apoptosis (strength 0.83, FDR $1.9e-04$, pink) and regulation of cell differentiation pathways (strength 0.87, FDR $4.28e-05$, yellow). In the progression time point notably we see significant enrichment in BCR signaling (strength 1.87, FDR $2.58e-12$, red) and MAPK signaling (strength 1.31, FDR $7.00e-05$, purple) involving the genes BTK, MAPK1, KRAS and NRAS. Upregulation of BCR signaling has been associated with Venetoclax progression with activation of the downstream MAPK signaling pathways [7,15]. Furthermore, there was also enrichment of Nf kappa B signaling pathways which included the genes TRAF3 and NFKBIE (strength 1.44, FDR $8.7e-4$, yellow) and regulation of cell cycle (strength 0.85, FDR 0.0058, green). These results show the ability of our harmonic framework to extract clinically/biological plausible gene sets supported by the existing literature [7,15] and their clinical findings offering a measure of validation. Furthermore, highlighted and pointed out new element that could lead to new discoveries.

4 Conclusion

In this paper, we introduce a framework using Harmonic Persistent Homology to extract and integrate information from multi-omics data that enables the discovery of hidden structure in the data that are clinically plausible. The use of harmonic weights in persistent homology allows the information of the spatial structure of the data to be mapped back to the features in the data. On top of this, it also reveals *essential* simplices which encode the significant biologically relevant relationships. This approach can have direct therapeutic implications since they can highlight possible new insight as demonstrated in our results.

5 Acknowledgements

DG carried out this work during an internship at IBM T J Watson Research Center. SB was partially supported by NSF grants CCF-1910441 and CCF-2128702. We are very grateful to Aishath Naeem for her insight in interpreting the CLL patient results. The results shown here are in whole or part based upon data generated by the TCGA Research Network: <https://www.cancer.gov/tcga>.

6 Availability and Implementation

Source code, user manual, and sample input-output sets are available for downloading at <https://github.com/IBM/matilda>.

References

1. Basu, S., Cox, N.: Harmonic persistent homology (extended abstract). In: 2021 IEEE 62nd Annual Symposium on Foundations of Computer Science—FOCS 2021, pp. 1112–1123. IEEE Computer Soc., Los Alamitos, CA ([2022] ©2022). <https://doi.org/10.1109/FOCS52979.2021.00110>, <https://doi.org/10.1109/FOCS52979.2021.00110>
2. Basu, S., Utro, F., Parida, L.: Essential Simplices in Persistent Homology and Subtle Admixture Detection. In: Parida, L., Ukkonen, E. (eds.) 18th International Workshop on Algorithms in Bioinformatics (WABI 2018). Leibniz International Proceedings in Informatics (LIPIcs), vol. 113, pp. 14:1–14:10. Schloss Dagstuhl–Leibniz-Zentrum fuer Informatik, Dagstuhl, Germany (2018). <https://doi.org/10.4230/LIPIcs.WABI.2018.14>, <http://drops.dagstuhl.de/opus/volltexte/2018/9316>
3. Bose, A., Platt, D.E., Haiminen, N., Parida, L.: Cuna: Cumulant-based network analysis of genotype-phenotype associations in parkinson’s disease. medRxiv (2021). <https://doi.org/10.1101/2021.08.02.21261457>, <https://www.medrxiv.org/content/early/2021/08/05/2021.08.02.21261457>
4. Edelsbrunner, H., Harer, J.L.: Computational topology: an introduction. American Mathematical Society (2022)
5. Hasin, Y., Seldin, M., Lusis, A.: Multi-omics approaches to disease. *Genome biology* **18**(1), 1–15 (2017)
6. Jia, R., Li, Z., Liang, W., Ji, Y., Weng, Y., Liang, Y., Ning, P.: Identification of key genes unique to the luminal a and basal-like breast cancer subtypes via bioinformatic analysis. *World Journal of Surgical Oncology* **18**(1), 1–11 (Dec 2020). <https://doi.org/10.1186/s12957-020-02042-z>, <https://wjso.biomedcentral.com/articles/10.1186/s12957-020-02042-z>, number: 1 Publisher: BioMed Central
7. Khalsa, J.K., Cha, J., Utro, F., Naeem, A., Murali, I., Kuang, Y., Vasquez, K., Li, L., Tyekucheva, S., Fernandes, S.M., Veronese, L., Guieze, R., Sasi, B.K., Wang, Z., Machado, J.H., Bai, H., Alasfour, M., Rhrissorrakrai, K., Levovitz, C., Danysh, B.P., Slowik, K., Jacobs, R.A., Davids, M.S., Pawletz, C.P., Leshchiner, I., Parida, L., Getz, G., Brown, J.R.: Genetic events associated with venetoclax resistance in CLL identified by whole-exome sequencing of patient samples. *Blood* **142**(5), 421–433 (08 2023). <https://doi.org/10.1182/blood.2022016600>, <https://doi.org/10.1182/blood.2022016600>
8. Liao, T., Wei, Y., Luo, M., Zhao, G.P., Zhou, H.: tmap: an integrative framework based on topological data analysis for population-scale microbiome stratification and association studies. *Genome biology* **20**, 1–19 (2019)
9. Libbrecht, M.W., Noble, W.S.: Machine learning applications in genetics and genomics. *Nature Reviews Genetics* **16**(6), 321–332 (2015)
10. Parry, E.M., Leshchiner, I., Guièze, R., Johnson, C., Tausch, E., Parikh, S.A., Lemvigh, C., Broséus, J., Hergalant, S., Messer, C., Utro, F., Levovitz, C., Rhrissorrakrai, K., Li, L., Rosebrock, D., Yin, S., Deng, S., Slowik, K., Jacobs, R., Huang, T., Li, S., Fell, G., Redd, R., Lin, Z., Knisbacher, B.A., Livitz, D., Schneider, C., Ruthen, N., Elagina, L., Taylor-Weiner, A., Persaud, B., Martinez, A., Fernandes, S.M., Purroy, N., Anandappa, A.J., Ma, J., Hess, J., Rassenti, L.Z., Kipps, T.J., Jain, N., Wierda, W., Cymbalista, F., Feugier, P., Kay, N.E., Livak, K.J., Danysh, B.P., Stewart, C., Neuberg, D., Davids, M.S., Brown, J.R., Parida, L., Stilgenbauer, S., Getz, G., Wu, C.J.: Evolutionary history of transformation from chronic lymphocytic leukemia to richter syndrome. *Nat. Med.* **29**(1), 158–169 (Jan 2023)
11. Platt, D., Bose, A., Levovitz, C., Rhrissorrakrai, K., Parida, L.: Epidemiological topology data analysis links severe covid-19 to raas and hyperlipidemia associated metabolic syndrome conditions. medRxiv (2022). <https://doi.org/10.1101/2022.03.31.22273239>, <https://www.medrxiv.org/content/early/2022/04/03/2022.03.31.22273239>
12. Platt, D.E., Basu, S., Zalloua, P.A., Parida, L.: Characterizing redescription using persistent homology to isolate genetic pathways contributing to pathogenesis. *BMC Systems Biology* **10**(1), S10 (Jan 2016). <https://doi.org/10.1186/s12918-015-0251-2>
13. Szklarczyk, D., Gable, A.L., Nastou, K.C., Lyon, D., Kirsch, R., Pyysalo, S., Doncheva, N.T., Legeay, M., Fang, T., Bork, P., Jensen, L.J., von Mering, C.: The STRING database in 2021: customizable protein–protein networks, and functional characterization of user-uploaded gene/measurement sets. *Nucleic Acids Res.* **49**(D1), D605–D612 (Jan 2021)
14. Székely, G.J., Rizzo, M.L., Bakirov, N.K.: Measuring and testing dependence by correlation of distances. *The Annals of Statistics* **35**(6), 2769–2794 (Dec 2007). <https://doi.org/10.1214/009053607000000505>, <https://projecteuclid.org/journals/annals-of-statistics/volume-35/issue-6/Measuring-and-testing-dependence-by-correlation-of-distances/10.1214/009053607000000505.full>, publisher: Institute of Mathematical Statistics
15. Thompson, P.A., Wierda, W.G.: Eliminating minimal residual disease as a therapeutic end point: working toward cure for patients with CLL. *Blood* **127**(3), 279–286 (01 2016). <https://doi.org/10.1182/blood-2015-08-634816>, <https://doi.org/10.1182/blood-2015-08-634816>
16. Vipond, O., Bull, J.A., Macklin, P.S., Tillmann, U., Pugh, C.W., Byrne, H.M., Harrington, H.A.: Multiparameter persistent homology landscapes identify immune cell spatial patterns in tumors. *Proceedings of the National Academy of Sciences* **118**(41), e2102166118 (2021)

17. Zheng, F., Zhang, S., Churas, C., Pratt, D., Bahar, I., Ideker, T.: Hidedf: identifying persistent structures in multiscale ‘omics data. *Genome biology* **22**(1), 1–15 (2021)

Supplementary Material

S1 Gene list

Here is the gene list used for the analysis in Section 3.1: GRM4, GRM8, KRT18, NMUR1, MUC1, CX3CL1, GATA3, NCAM1, CENPI, CENPK, CDC7, CCNE2, KIF18A, STIL, CDCA7, CKS2

Here the gene list used for the analysis in Section 3.4: GNB1, DNAJC11, MTOR, SPEN, ARID1A, FUBP1, NRAS, ITPKB, XPO1, ATF2, FSIP2, SF3B1, PLCL1, IRS1, MYD88, SETD2, KLHL6, FBXW7, TLR2, KIAA0947, ITGA1, ITGA2, SKIV2L2, PIK3R1, ANKHD1, IRF4, HIST1H1E, HIST1H1B, PIM1, NFKBIE, ZNF292, SYNE1, CARD11, POT1, C7orf55-LUC7L2, BRAF, LYN, CDKN2A, SYK, NOTCH1, TRAF2, EGR2, PLCE1, NFKB2, PLEKHA1, NXF1, INPPL1, BIRC3, ATM, CCND2, CDKN1B, PLCZ1, KRAS, KMT2D, BAZ2A, POLR3B, PTPN11, XPO4, FOS, PPP2R5C, TRAF3, MGA, PDIA3, MAP2K1, CHD2, CREBBP, SETD1A, NFAT5, PLCG2, ZC3H18, TP53, MED1, IKZF3, CD79B, BCL2, NFATC1, RPS15, CD79A, BAX, CNOT3, ASXL1, SAMHD1, DYRK1A, MAPK1, IGLL5, CHEK2, EWSR1, BCOR, DDX3X, MED12, ZMYM3, ATRX, BTK, NKAP, ELF4, IRAK1, FAM50A, BRCC3